

Cobalt 1,3-Diisopropyl-1*H*-imidazol-2-ylidene Complexes: Synthesis, Solid-State Structures, and Quantum Chemistry Calculations

Carmen L. Vélez,[†] Phineus R. L. Markwick,^{*,†,‡} Ryan L. Holland,[†]
Antonio G. DiPasquale,[†] Arnold L. Rheingold,[†] and Joseph M. O'Connor^{*,†}

[†]Department of Chemistry and Biochemistry, University of California, San Diego, 9500 Gilman Drive, MC 0358, La Jolla, California 92093-0358, United States, and [‡]Howard Hughes Medical Institute, United States

Received July 12, 2010

The reaction of ($\eta^5\text{-C}_5\text{H}_5$)Co(PPh₃)₂ (**1**) with 1,3-bis(isopropyl)imidazol-2-ylidene (ImⁱPr₂, **17**) leads to the formation of ($\eta^5\text{-C}_5\text{H}_5$)Co(PPh₃)(ImⁱPr₂) (**5**) in 69% yield. N-Heterocyclic carbene **17** also undergoes reaction with ($\eta^5\text{-C}_5\text{H}_5$)Co(CO)₂ (**9**) to give ($\eta^5\text{-C}_5\text{H}_5$)Co(ImⁱPr₂)(CO) (**6**) in 30% yield. The barrier to rotation about the Co—C^{carbene} bond in **6** has been determined by variable-temperature ¹H NMR spectroscopy (13.6 kcal/mol) and by computation (13.3 kcal/mol). Complex **5** undergoes reaction with PhSSPh to give the paramagnetic thiolato complex ($\eta^5\text{-C}_5\text{H}_5$)Co(ImⁱPr₂)(SPh) (**7**), which is oxidized to the metallosulfone complex ($\eta^5\text{-C}_5\text{H}_5$)Co(ImⁱPr₂)(SO₂Ph) (**8**). The solid-state structures of **5**–**8** were determined by X-ray crystallography. The structural and dynamic properties of **6**, ($\eta^5\text{-C}_5\text{H}_5$)Co(ImMe₂)(CO) (ImMe₂ = 1,3-dimethylimidazol-2-ylidene), and ($\eta^5\text{-C}_5\text{H}_5$)-Co(ImAr₂)(CO) (ImAr₂ = 1,3-dimesityl-2-ylidene) were examined by quantum chemistry calculations.

Introduction

The conversion of ($\eta^5\text{-C}_5\text{H}_5$)Co(PPh₃)₂ (**1**) and TMSC≡C(SOTol) to the cobaltosulfoxide complex ($\eta^5\text{-C}_5\text{H}_5$)Co-(PPh₃)₂{S(=O)Tol}(C≡CTMS) (**2**, Tol = *p*-C₆H₄Me) represents the first unambiguous example of sulfoxide carbon-sulfur bond activation (Scheme 1).¹ In the presence of oxygen, complex **2** underwent conversion to cobaltosulfone complex ($\eta^5\text{-C}_5\text{H}_5$)Co(PPh₃)₂{S(=O)₂Tol}(C≡CTMS) (**3**), whereas heating solutions of **2** in the absence of oxygen led to the formation of O=PPh₃ and the thiolato-bridged complexes [$\eta^5\text{-C}_5\text{H}_5$]Co(μ - η^2 -STol)₂₂ (**4**-eq,ax and **4**-eq,eq). In an effort to stabilize **2** with respect to formation of **4**, we sought to prepare analogues in which the phosphine ligand was replaced by an N-heterocyclic carbene ligand. N-Heterocyclic carbene (NHC) ligands afford significant advantages over phosphine ligands with respect to ligand donor properties and oxidative stability.² Here we report the synthesis and characterization of the cobalt 1,3-bis(isopropyl)-imidazol-2-ylidene (ImⁱPr₂) complexes ($\eta^5\text{-C}_5\text{H}_5$)Co-(ImⁱPr₂)(PPh₃) (**5**) and ($\eta^5\text{-C}_5\text{H}_5$)Co(ImⁱPr₂)(CO) (**6**) and conversion of **5** to ($\eta^5\text{-C}_5\text{H}_5$)Co(ImⁱPr₂)(SC₆H₅) (**7**) and ($\eta^5\text{-C}_5\text{H}_5$)Co(ImⁱPr₂)(SO₂C₆H₅) (**8**).

Results and Discussion

Synthesis and Spectroscopic Characterization of ($\eta^5\text{-C}_5\text{H}_5$)-Co(ImⁱPr₂)(L) (**5**, L = PPh₃; **6**, L = CO). The earliest

preparations of cobalt NHC complexes involved the reactions of low-valent cobalt precursors with electron-rich alkenes, as shown below for the conversion of ($\eta^5\text{-C}_5\text{H}_5$)Co(CO)₂ (**9**) to ($\eta^5\text{-C}_5\text{H}_5$)Co(CO)[=C(NMe)CH₂CH₂(NMe)] (**10**; eq 1).^{3,4} More recently, access to stable organic carbenes,⁵ such as **11**–**13**, has led to the preparation of cobalt NHC complexes **14**–**16** from ligand substitution chemistry (eqs 2 and 3).^{6–8} Butenschön's observation that **14** was formed by substitution of a phosphine ligand suggested that the readily available bis(phosphine) complex ($\eta^5\text{-C}_5\text{H}_5$)Co(PPh₃)₂ (**1**) may serve as a useful precursor to the first ($\eta^5\text{-C}_5\text{H}_5$)M(PPh₃)(NHC) (NHC = N-heterocyclic carbene) complexes. We therefore examined the room-temperature reaction of **1** (1.17 g, 1.8 mmol)⁸ with 1,3-bis(isopropyl)imidazol-2-ylidene (ImⁱPr₂, **17**; 3.61 mmol)⁹ and observed the formation of ($\eta^5\text{-C}_5\text{H}_5$)Co-(PPh₃)(ImⁱPr₂) (**5**), which was isolated as an air-sensitive dark blue powder in 69% yield (eq 4). In the ¹³C{¹H} NMR spectrum (C₆D₆) of **5**, the carbene carbon resonance is observed at 191.1 (d, *J*_{PC} = 32.3 Hz) ppm, which is upfield of the carbene carbon resonance observed for **10** (either 207.4 or 218.5 ppm) and **14** (241.4 ppm). In the ¹H NMR spectrum

(3) Lappert, M. F.; Pye, P. L. Carbene Complexes. 12. *J. Chem. Soc., Dalton Trans.* 1977, 21, 2172.

(4) For additional preparations of CpCo(NHC)(L) complexes from electron-rich alkenes see: (a) Macomber, D. W.; Rogers, R. D. *Organometallics* 1985, 4, 1485. (b) Delgado, S.; Moreno, C.; Macazaga, M. J. *Polyhedron* 1991, 10, 725.

(5) Bourissou, D.; Guerret, O.; Gabbai, F. P.; Bertrand, G. *Chem. Rev.* 2000, 100, 39.

(6) Foerstner, J.; Kakuschke, A.; Goddard, R.; Rust, J.; Wartchow, R.; Butenschön, H. *J. Organomet. Chem.* 2001, 617, 412.

(7) Fooladi, E.; Dalhus, B.; Tilset, M. *J. Chem. Soc., Dalton Trans.* 2004, 22, 3909.

(8) Simms, R. W.; Drewitt, M. J.; Baird, M. C. *Organometallics* 2002, 21, 2958.

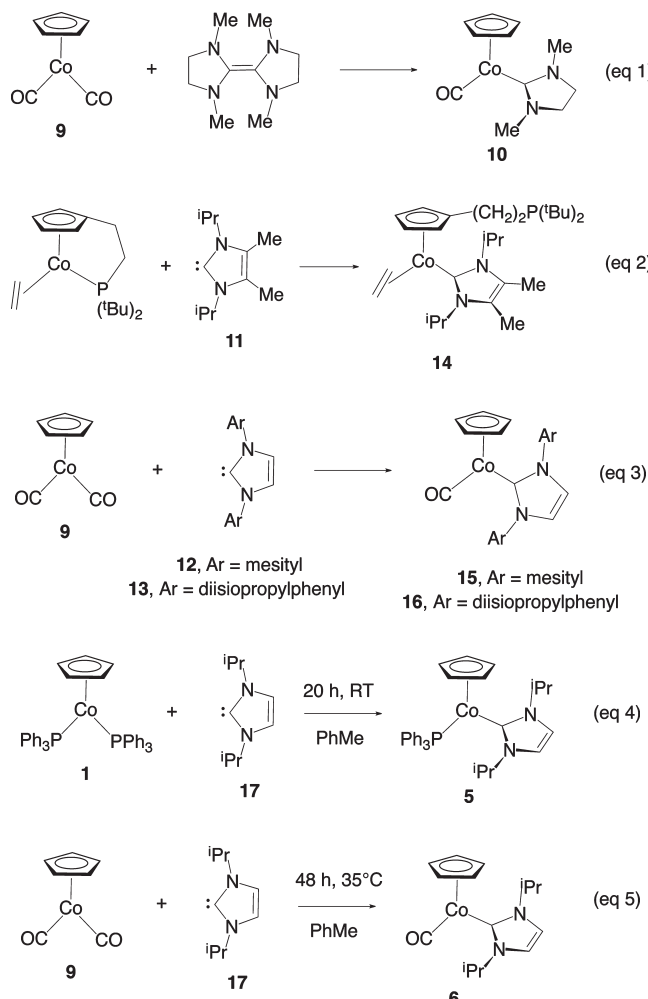
(9) Schaub, T.; Radius, U. *Chem.—Eur. J.* 2005, 11, 5024.

*To whom correspondence should be addressed. E-mail: jmoconnor@ucsd.edu.

(1) O'Connor, J. M.; Bunker, K. D.; Rheingold, A. L.; Zakharov, L. *J. Am. Chem. Soc.* 2005, 127, 4180.

(2) (a) Cruden, C. M.; Allen, D. P. *Coord. Chem. Rev.* 2004, 248, 2247. (b) Hahn, F. E.; Jahnke, M. C. *Angew. Chem., Int. Ed.* 2008, 47, 3122.

(benzene-*d*₆) of **5**, resonances attributed to the NHC ligand are observed at δ 6.54 (septet, $J_{\text{CH}} = 6.9$ Hz, 2H, NCHMe_2), 6.32 (s, 2H, $\text{NCH}=\text{CHN}$), 0.55 (d, $J_{\text{CH}} = 6.9$ Hz, 6H, $\text{NCH}(\text{CH}_3)_2$), and 1.04 (d, $J_{\text{CH}} = 6.9$ Hz, 6H, $\text{NCH}(\text{CH}_3)_2$). NHC ligands often exhibit rapid rotation about the metal–carbon bond due to weak back-bonding from the metal to the carbene carbon. For example, at room temperature in benzene-*d*₆, complex **14** exhibits a single doublet at δ 1.33 ($J_{\text{CH}} = 6.1$ Hz) for the 12 isopropyl-methyl hydrogens. In the case of **5**, the doublets at δ 0.55 and 1.04 ($\text{CH}(\text{CH}_3)_2$) remained unchanged over the temperature range 23–60 °C. The observation of one vinyl hydrogen resonance and two methyl hydrogen resonances for **5** is consistent with a structure in which the favored dihedral angle, θ , between the (Cp^{cnt})-Co-C^{carbene} plane and the N–C–N plane is approximately 90° (Figure 1). Saturation of the resonance at δ 4.74 led to a NOE at the 1.04 resonance, but not at the 0.55 resonance. Alternatively, saturation of the δ 1.04 resonance led to a NOE at the 4.74 C₅H₅ singlet. The δ 1.04 doublet is therefore assigned to the isopropyl methyl hydrogens that are *syn* to the C₅H₅ ligand, and the 0.55 doublet is assigned to the methyl groups that are *anti* to the C₅H₅ ligand.



Heating a toluene solution of ($\eta^5\text{-C}_5\text{H}_5$)Co(CO)₂ (**9**) (1.87 g, 1.04×10^{-2} mol) and Im*i*Pr₂ (**17**; 1.22 g, 8.01×10^{-3} mol, 0.40 M) under a nitrogen atmosphere at 35 °C for 2 days led to the formation of ($\eta^5\text{-C}_5\text{H}_5$)Co(Im*i*Pr₂)(CO) (**6**) in 30% isolated yield (eq 5). In the ¹³C{¹H} NMR spectrum (toluene-*d*₈) of **6**, resonances at 183.6 and 207.8 ppm are

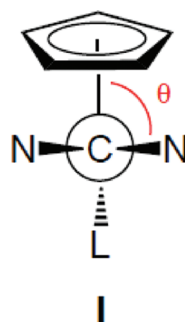
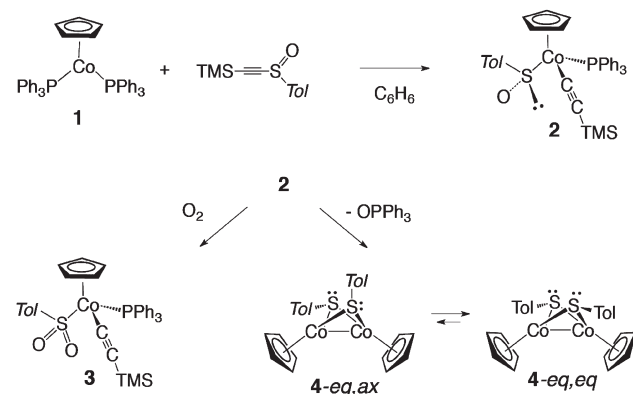


Figure 1. Definition of θ , the dihedral angle between the C₅H₅-centroid–Co–C^{carbene} and N–C–N planes in ($\eta^5\text{-C}_5\text{H}_5$)Co(Im*i*Pr₂)(L) complexes.

Scheme 1. Synthesis of Cobalt-Sulfenate (2), Sulfinate (3), and μ -Thiolato (4) Complexes



assigned to the carbon monoxide and carbene carbon bound to cobalt. In the IR spectrum (hexane) of **6**, the $\nu(\text{C=O})$ stretching frequency is observed at 1911 cm⁻¹, which is among the lowest values reported for cobalt carbonyl stretching frequencies in related NHC complexes, such as **10**^{4a} (1915 cm⁻¹, hexane), **15**⁷ (1921 cm⁻¹, hexane), and **16**⁸ (1921 cm⁻¹, hexane). All of these ($\eta^5\text{-C}_5\text{H}_5$)Co(NHC)(CO) complexes are significantly more electron rich than the triphenylphosphine analogue, ($\eta^5\text{-C}_5\text{H}_5$)Co(PPh₃)(CO) (1937 cm⁻¹, hexanes),¹⁰ and slightly more electron rich than ($\eta^5\text{-C}_5\text{H}_5$)Co(PMe₃)(CO) (1923 cm⁻¹, pentane).¹¹ The ¹H NMR spectrum (benzene-*d*₆) of **6** exhibits singlets at δ 4.87 (5H, C₅H₅) and 6.34 (2H, $\text{NCH}=\text{CHN}$) and a broad resonance at 1.01 (12H, $\text{NCH}(\text{CH}_3)_2$) indicative of hindered rotation about the Co–C^{carbene} bond on the NMR time scale. At -70 °C, the ¹H NMR spectrum (THF-*d*₈) of **6** exhibits two broad doublets at δ 1.01 ($J_{\text{HH}} = 5.35$ Hz, 6H) and 0.90 ($J_{\text{HH}} = 6.69$ Hz, 6H), which broaden as the temperature is increased and coalesce at 3.0 °C ($\Delta G^\ddagger > 13.6 (\pm 0.2)$ kcal/mol) (Figure 2). At +50 °C, a single doublet is observed for the 12 methyl hydrogens at δ 1.05 ($J_{\text{HH}} = 6.69$ Hz). To our knowledge, these results represent the first experimental determination of a barrier to rotation about the cobalt–carbon bond of a carbene ligand.

Solid-State Structures of ($\eta^5\text{-C}_5\text{H}_5$)Co(Im*i*Pr₂)(L) (5**, L = PPh₃; **6**, L = CO).** The solid-state structures of **5** and **6** were determined by X-ray crystallographic analyses (Figures 3 and 4, Table 1). Both structures assume distorted trigonal-planar coordination geometry defined by the C₅H₅-centroid

(10) Hart-Davis, A. J.; Graham, W. A. G. *Inorg. Chem.* **1970**, *9*, 2658.

(11) Spencer, A.; Werner, H. *J. Organomet. Chem.* **1979**, *171*, 219.

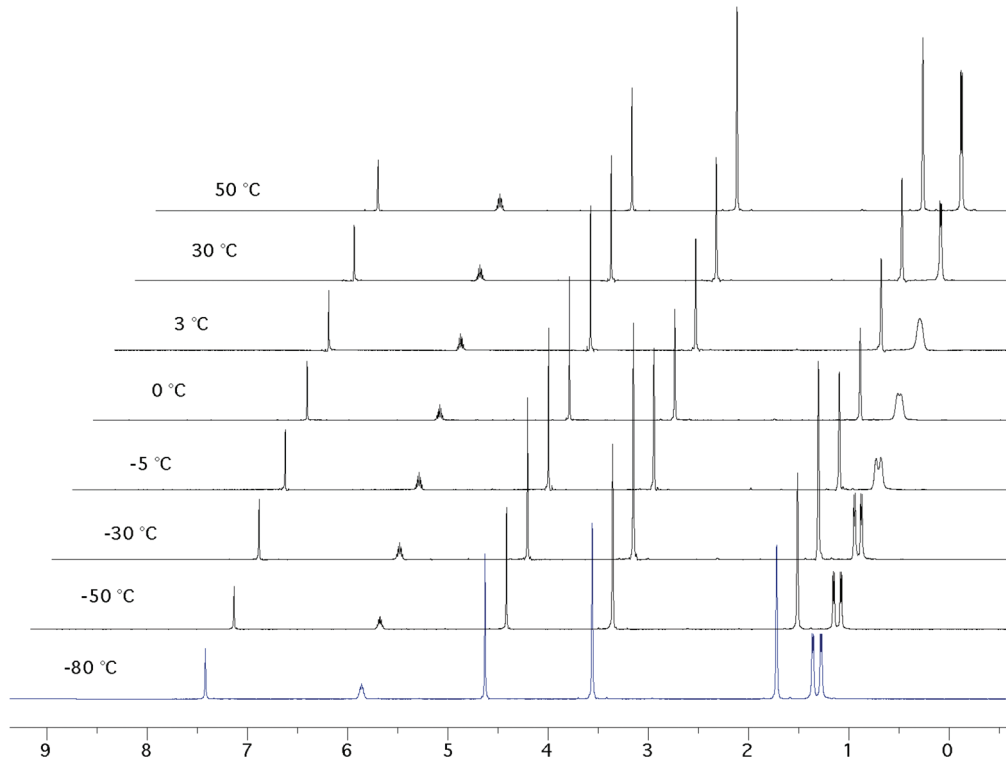


Figure 2. Variable-temperature NMR spectra (THF-*d*₈) for ($\eta^5\text{-C}_5\text{H}_5\text{Co}(\text{Im}'\text{Pr}_2)\text{(CO)}$) (**6**).

(Cp^{cnt}), the carbene carbon C(6), and L (PPh₃, CO). The $\text{Cp}^{\text{cnt}}\text{-Co-C}(6)$ angles are similar in magnitude for both structures and fall in the range 130–132°. However, the larger steric bulk of PPh₃ relative to CO results in substantially smaller $\text{Cp}^{\text{cnt}}\text{-Co-L}$ angles for **5** (L = PPh₃, 132°) than in the case of **6** (L = CO, 142°). For comparison, the $\text{Cp}^{\text{cnt}}\text{-Co-P}$ angles in ($\eta^5\text{-C}_5\text{H}_5\text{Co(PPh}_3)_2$) (**1**) are 130°.¹² The dihedral angle between the $\text{Cp}^{\text{cnt}}\text{-Co-C}(6)$ and N-C(6)-N planes (θ , Figure 1) in **5** (98°) and **6** (92°) is much larger than that observed for the 1,3-diarylimidazol-2-ylidene complexes **15** (45°)⁷ and **16** (46°)⁸ (Figure 5). Both **15** and **16** presumably adopt a conformation that minimizes the steric congestion between the aryl nitrogen substituents and the cyclopentadienyl ligand. Despite the more electron-rich metal center and greater steric congestion in phosphine complex **5**, the Co-C(6)^{carbene} distance in **5** (1.880(2) Å) is slightly shorter than in **6** (1.898(2) Å). The same trend is found for the Co-Cp^{cnt} distances, which are 1.700(1) Å for **5** and 1.6723(1) Å for **6**.

Computational Studies on ($\eta^5\text{-C}_5\text{H}_5\text{Co}(\text{Im}'\text{Pr}_2)\text{(CO)}$) (6**).** N-Heterocyclic carbene ligands are typically viewed as pure σ -donors with minimal π -acceptor properties. There is, however, both experimental and computational evidence suggesting that certain electron-rich metals may engage in back-bonding to the NHC ligand.¹³ There are also literature reports that suggest that in some cases NHC ligands are capable of π -donation to metals.¹⁴ In order to further study the structural dynamic properties of ($\eta^5\text{-C}_5\text{H}_5\text{Co(NHC)L}$) systems, we performed a series of quantum chemistry

(12) Hoffmann, F.; Wagler, J.; Roewer, G. *Z. Anorg. Allg. Chem.* **2008**, *634*, 1133.

(13) Penka, E. F.; Schläpfer, C. W.; Atanasov, M.; Albrecht, M.; Daul, C. *J. Organomet. Chem.* **2007**, *692*, 5709, and references therein.

(14) Khramov, D. M.; Lynch, V. M.; Bielawski, C. W. *Organometallics* **2007**, *26*, 6042, and references therein.

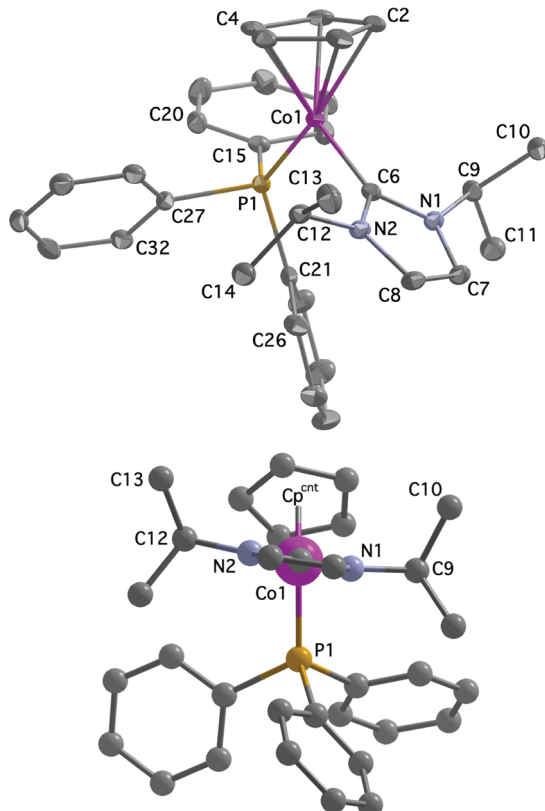


Figure 3. ORTEP structure of **5** (upper frame) and view of the dihedral angle ($\theta=98^\circ$) between the $\text{Cp}^{\text{cnt}}\text{-Co-C}(6)$ and N(1)-C(6)-N(2) planes for **5** (lower frame). Hydrogen atoms have been omitted for clarity.

calculations on **6**. The aim of this study was to identify the relative contributions arising from electronic and steric effects

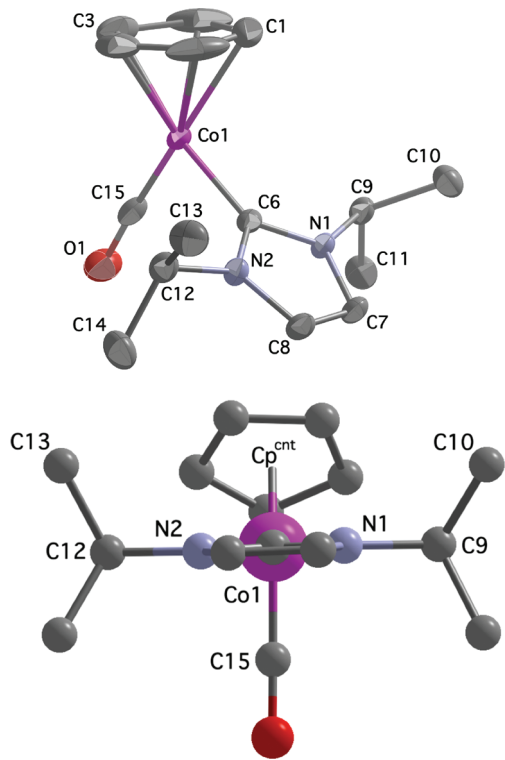
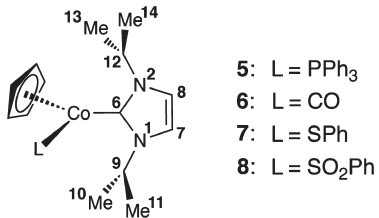


Figure 4. Solid-state molecular structures of **6** (upper frame) and view of dihedral angle ($\theta = 92^\circ$) between the Cp^{cnt} -Co-C(6) and N(1)-C(6)-N(2) planes for **6** (lower frame). Hydrogen atoms have been omitted for clarity.

Table 1. Selected Bond Distances (Å) and Angles (deg) for 5–8



	5	6	7	8
Co-Cp	1.700	1.732	1.732	1.710
Co-C(6)	1.880(2)	1.898(2)	1.919(2)	1.922(2)
Co-L	2.1015(7)	1.698(2)	2.1910(13)	2.1741(6)
C(6)-N(1)	1.372(3)	1.362(3)	1.365(3)	1.355(3)
C(6)-N(2)	1.372(3)	1.365(3)	1.372(3)	1.356(3)
N(1)-C(7)	1.383(3)	1.381(3)	1.388(3)	1.385(3)
N(2)-C(8)	1.387(3)	1.388(3)	1.396(3)	1.385(3)
C(7)-C(8)	1.345(3)	1.343(3)	1.349(3)	1.335(3)
N(1)-C(9)	1.474(3)	1.476(3)	1.479(3)	1.473(3)
N(2)-C(12)	1.479(3)	1.472(3)	1.480(3)	1.479(3)
Cp-Co-C(6)	131.54	130.23	129.51	131.27
Cp-Co-L	131.62	142.41	141.21	132.03
C(6)-Co-L	96.83(6)	87.35(9)	89.27(7)	96.48(6)
Co-C(6)-N(1)	128.09(16)	128.24(16)	129.39(17)	128.87(16)
Co-C(6)-N(2)	128.83(17)	127.59(16)	126.64(16)	126.58(16)
N1-C(6)-N(2)	103.08(18)	104.15(18)	103.86(19)	104.35(19)

that determine the specific conformation of the NHC ligand in $(\eta^5\text{-C}_5\text{H}_5)\text{Co}(\text{NHC})\text{L}$ complexes.

A full geometry optimization was initially performed on **6**, and the resulting optimized structure (**6**-*calc*, Figure 6) was remarkably similar to the X-ray crystal structure (Figure 4).

The geometry-optimized carbene carbon–cobalt bond is 1.902 Å compared to the X-ray crystal structure (1.898 Å). Similarly, the two C–Co–C–N dihedral angles are $\{-90.164^\circ, 91.177^\circ\}$ and $\{-86.635^\circ, 89.295^\circ\}$ for the DFT-optimized geometries and the X-ray crystal structures, respectively. Using the geometry-optimized structure, the molecular orbitals for the two interacting fragments ($\eta^5\text{-C}_5\text{H}_5$)-Co(CO) and NHC were calculated and analyzed. Figure 6 shows the principal molecular orbitals involved in the binding interaction between the $(\eta^5\text{-C}_5\text{H}_5)\text{Co}(\text{CO})$ and NHC ligand in the bound complex structure. The primary interaction is between the NHC HOMO and the $(\eta^5\text{-C}_5\text{H}_5)\text{Co}(\text{CO})$ LUMO, and, as is well understood, the carbene carbon acts as a strong σ -donor. Analysis of the other molecular orbitals shows no further significant electronic interaction effects. Most notably, the unoccupied molecular orbitals for the NHC ligand are extremely diffuse and are located on the opposite side of the ligand of the $(\eta^5\text{-C}_5\text{H}_5)\text{Co}(\text{CO})$ -interaction site, confirming that NHC is a poor π -acceptor (Figures S1 and S2). Additionally, analysis of the NHC HOMO–1 molecular orbital reveals that the carbene carbon is also a poor π -donor.

Analysis of the individual molecular orbitals suggests that the specific orientation of the ImⁱPr₂ ligand in the complex is determined predominantly, if not solely, by steric effects. In order to substantiate this result, a series of partial geometry optimizations were performed on **6**-*calc* in which the C–Co–C–N dihedral angle was treated as a constraint and systematically varied from -80° to -190° (see Methods for more details). The upper panel of Figure 7 shows the energy of the system as a function of the C–Co–C–N dihedral angle. The energy barrier for rotation of the Co–ImⁱPr₂ bond is found to be 13.3 kcal/mol, which is in extremely good agreement with the simulated NMR data result of 13.6 kcal/mol. As the ImⁱPr₂ ligand is rotated away from the optimal geometry (at -90.164°), the system exhibits many structural distortions: The carbene carbon–cobalt bond length increases from 1.902 Å to 1.960 Å (as shown in the lower panel of Figure 7). The O–C–Co angle distorts away from a near-linear geometry (178.7°) to 170.2° as the CO group tilts away from the rotating ImⁱPr₂ ligand. Similarly, steric interaction between the ImⁱPr₂ and C₅H₅ ligands causes the C₅H₅ ring to tilt relative to the cobalt atom (see Supporting Information for more details).

The observed structural distortions of the complex discussed above provide further evidence that steric effects determine the preferential geometry of the NHC ligand predominantly. This result is confirmed by a second, identical set of QC calculations performed on $(\eta^5\text{-C}_5\text{H}_5)\text{Co}(\text{ImMe}_2)(\text{CO})$, where ImMe₂ is the 1,3-dimethylimidazol-2-ylidene ligand (data not shown). The energy barrier to rotation about the Co–ImMe₂ bond is found to be only 8.7 kcal/mol, which represents a 35% decrease in the energy barrier to rotation compared to the more bulky ImⁱPr₂ ligand. The results of this study suggest that the specific orientation of the NHC ligand in $(\eta^5\text{-C}_5\text{H}_5)\text{Co}(\text{NHC})\text{CO}$ systems is determined solely by steric interactions. This is obviously also true for extremely bulky NHC ligands, such as the mesityl-substituted NHC ligand in **15**. The QC-optimized geometry of this system afforded a C–Co–C–N dihedral angle of 57.3° compared to the X-ray crystal structure (46.4°). This 10° discrepancy between the theoretical and experimental result is the product of an exceedingly shallow potential energy well about the optimal geometry.

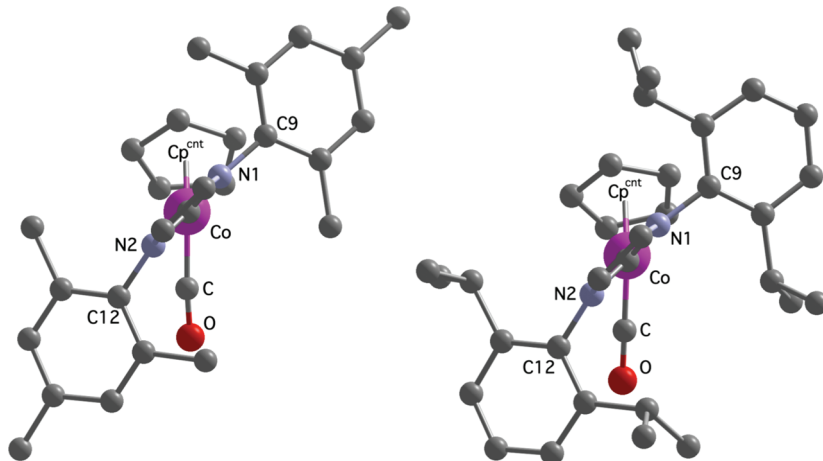


Figure 5. Solid-state molecular structures of **15** (left, $\theta = 45^\circ$)⁷ and **16** (right, $\theta = 46^\circ$)⁸ highlighting the dihedral angle (θ) between the $\text{Cp}^{\text{cnt}}\text{--Co--C}(6)$ and $\text{N}(1)\text{--C}(6)\text{--N}(2)$ planes. Hydrogen atoms have been omitted for clarity.

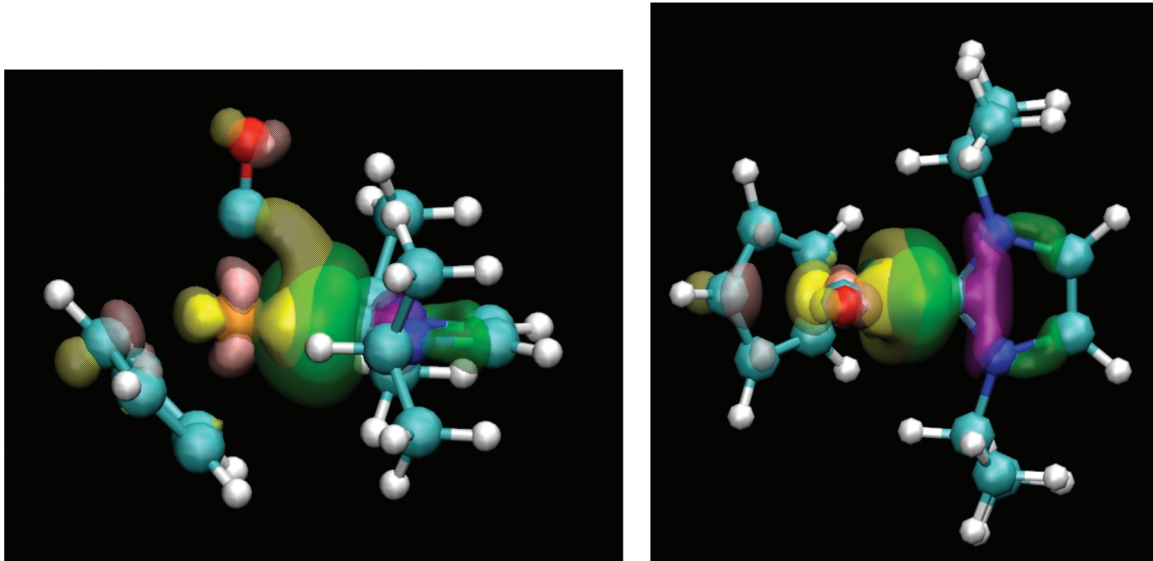


Figure 6. Orthogonal views of the molecular orbitals defining the primary electronic interaction between $(\eta^5\text{-C}_5\text{H}_5)\text{Co}(\text{CO})$ and $\text{Im}'\text{Pr}_2$ in **6**-*calc*. The positive and negative phases of the $\text{Im}'\text{Pr}_2$ HOMO are depicted in green and purple; the phases of the $(\eta^5\text{-C}_5\text{H}_5)\text{Co}(\text{CO})$ LUMO are depicted in yellow and pink. Two contour plots are displayed for each normalized MO, the solid surface is the contour at ± 0.1 , and the transparent surface is the contour at ± 0.05 .

We consider that this is due to the large inherent flexibility of this particular NHC ligand; however crystal packing effects and possible errors in the treatment of the dispersion forces in the DFT calculations cannot be ruled out.

Synthesis and Spectroscopic Characterization of $(\eta^5\text{-C}_5\text{H}_5)\text{Co}(\text{Im}'\text{Pr}_2)(\text{L})$ (7, $\text{L} = \text{SOPh}$; 8, $\text{L} = \text{SO}_2\text{Ph}$). Attempts to observe carbon–sulfur bond activation in the reaction of **5** and $\text{TMSC}\equiv\text{C}(\text{SOTol})$ have thus far proved unproductive. In an effort to prepare $(\eta^5\text{-C}_5\text{H}_5)\text{Co}(\text{Im}'\text{Pr}_2)$ complexes of sulfur-based ligands, we examined the reactions of **5** with diphenyl disulfide (PhSSPh) and benzenesulfonothioic acid, PhSSO_2Ph (Scheme 2). Following a similar procedure to that utilized by Macomber for the conversion of the less sterically congested NHC complex $(\eta^5\text{-C}_5\text{H}_5)\text{Co}(\text{H}_2\text{ImMe}_2)(\text{CO})$ ($\text{H}_2\text{ImMe}_2 = 1$, 3-dimethylimidazolin-2-ylidene) to the corresponding thiolato complex $(\eta^5\text{-C}_5\text{H}_5)\text{Co}(\text{ImMe}_2)(\text{SPh})$ (**18**)^{4a} complex **5** underwent reaction with diphenyl disulfide to give $(\eta^5\text{-C}_5\text{H}_5)\text{Co}(\text{Im}'\text{Pr}_2)(\text{SPh})$ (**7**), which was isolated as an orange crystalline solid in 87% yield. Complex **7** is paramagnetic with

$\mu_{\text{eff}} = 1.73 \mu_B$, as measured by Evans' NMR method. For **18**, $\mu_{\text{eff}} = 2.2 \mu_B$ and for cobaltocene $\mu_{\text{eff}} = 1.73 \mu_B$.^{4a} In the ^1H NMR spectrum (C_6D_6) of **7** broad resonances were observed at δ 3.2 and 11.5. The structure of **7** was unambiguously determined by a crystal structure analysis (Figure 8, Table 1). The conversion of **5** and Ph_2S_2 to monothiolato complex **7** contrasts with the reaction of $(\eta^5\text{-C}_5\text{H}_5)\text{Co}(\text{PMe}_3)(\text{CO})$ and Ph_2S_2 to give the dithiolato complex $(\eta^5\text{-C}_5\text{H}_5)\text{Co}(\text{PMe}_3)(\text{SPh})_2$.¹⁵ The different reaction outcomes are presumably due to the relative steric bulk of PMe_3 and $\text{Im}'\text{Pr}_2$.

Attempts to oxidize **7** to the corresponding cobaltosulf oxide complex by treatment with $(1S)\text{-(+)-(10-camphorsulfonyl)oxaziridine}$ led only to the isolation of the cobaltosulfone complex $(\eta^5\text{-C}_5\text{H}_5)\text{Co}(\text{SO}_2\text{Ph})(\text{Im}'\text{Pr}_2)$ (**8**) in 48% yield. Alternatively, when **5** was treated with benzenesulfonothioic acid (PhSO_2SPh), a mixture of **7** and **8** was formed, as determined by ^1H NMR spectroscopy. In the ^1H NMR

(15) Werner, H.; Juthani, B. *J. Organomet. Chem.* **1981**, 209, 211.

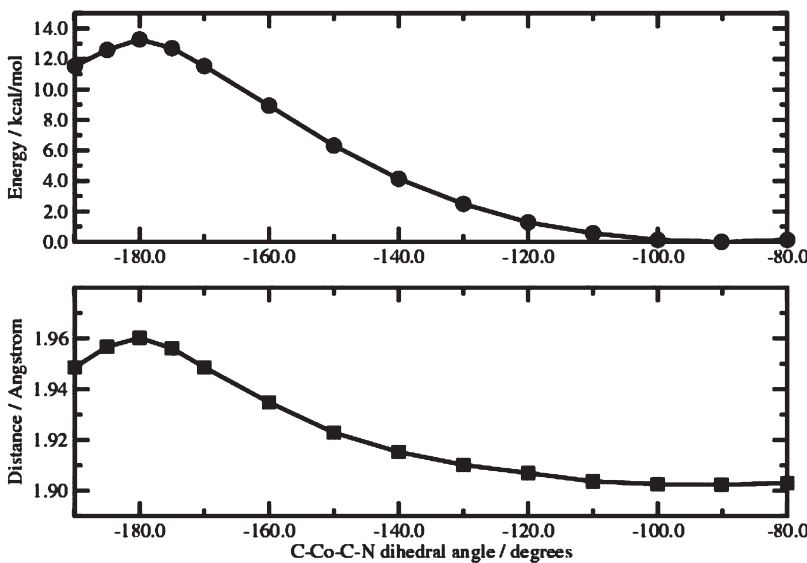
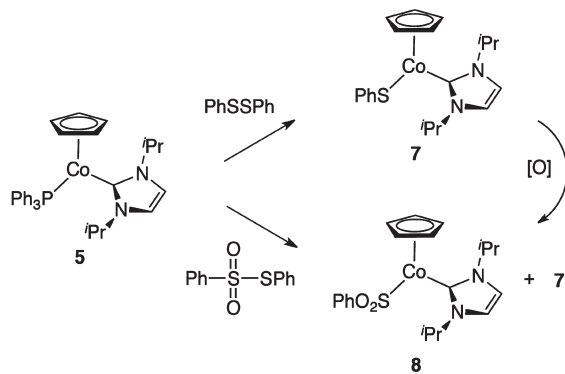


Figure 7. Variation of the enthalpy (upper panel) and Co–C(carbene) interatomic distance (lower panel) of **6-calc** as a function of the C–Co–C–N dihedral angle.

Scheme 2. Synthesis of ($\eta^5\text{-C}_5\text{H}_5$) $\text{Co}(\text{Im}^i\text{Pr}_2)(\text{SPh})$ (7**) and ($\eta^5\text{-C}_5\text{H}_5$) $\text{Co}(\text{Im}^i\text{Pr}_2)(\text{SO}_2\text{Ph})$ (**8**)**



spectrum (C_6D_6) of **8** broad resonances were observed at δ 5.6 and 12.8. Orange crystals of **8** were obtained from this mixture, and the solid-state structure was determined by X-ray crystallography (Figure 9, Table 1). As was the case for **5** and **6**, complexes **7** and **8** assume a distorted trigonal-planar coordination geometry defined by the C_5H_5 -centroid (Cp^{cnt}), the carbene carbon C(6), and L (SPh, or SO₂Ph). The $\text{Cp}^{\text{cnt}}\text{-Co-C}(6)$ angles are similar in magnitude for all four structures and fall in the range 130–132°. The larger steric bulk of PPh₃ and SO₂Ph, relative to CO and SPh, results in substantially smaller $\text{Cp}^{\text{cnt}}\text{-Co-L}$ angles for **5** (L = PPh₃, 132°) and **8** (L = SO₂Ph, 132°) than in the case of **6** (L = CO, 142°) and **7** (L = SPh, 141°). The dihedral angle between the $\text{Cp}^{\text{cnt}}\text{-Co-C}(6)$ and N–C(6)–N planes (θ , Figure 1) in **5** (98°), **6** (92°), **7** (77°), and **8** (85°) is much larger than that observed for the 1,3-diarylimidazol-2-ylidene complexes **15** (45°) and **16** (46°). Both **15** and **16** presumably adopt a conformation that minimizes the steric congestion between the aryl nitrogen substituents and the cyclopentadienyl ligand. Despite the more electron-rich metal center and greater steric congestion in phosphine complex **5**, the Co–C(6)^{carbene} distance in **5** (1.880(2) Å) is slightly shorter than in **6** (1.898(2) Å). The same trend is found for the Co–Cp^{cnt} distances, which are 1.700(1) Å for **5** and 1.6723(1) Å for **6**.

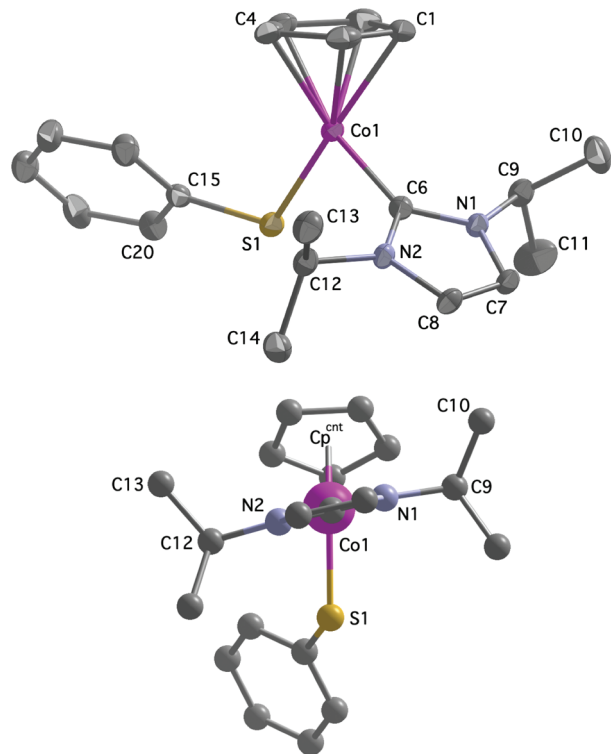


Figure 8. Solid-state molecular structures of **7** (upper frame) and view of dihedral angle ($\theta = 77^\circ$) between the $\text{Cp}^{\text{cnt}}\text{-Co-C}(6)$ and N(1)–C(6)–N(2) planes for **7** (lower frame). Hydrogen atoms have been omitted for clarity.

Conclusions

The reactions of ($\eta^5\text{-C}_5\text{H}_5$) $\text{Co}(\text{PPh}_3)_2$ (**1**) and ($\eta^5\text{-C}_5\text{H}_5$) $\text{Co}(\text{CO})_2$ (**10**) with 1,3-bis(isopropyl)imidazol-2-ylidene (ImⁱPr₂, **17**) lead to the formation of ($\eta^5\text{-C}_5\text{H}_5$) $\text{Co}(\text{PPh}_3)$ (ImⁱPr₂) (**5**) and ($\eta^5\text{-C}_5\text{H}_5$) $\text{Co}(\text{Im}^i\text{Pr}_2)(\text{CO})$ (**6**), respectively. Complex **5** is the first example of a cobalt triad ($\eta^5\text{-C}_5\text{H}_5$)-M(PPh₃)(NHC) complex, whereas **6** is the first cobalt–carbene complex for which the barrier to rotation about the cobalt–carbon has been experimentally determined. The measured

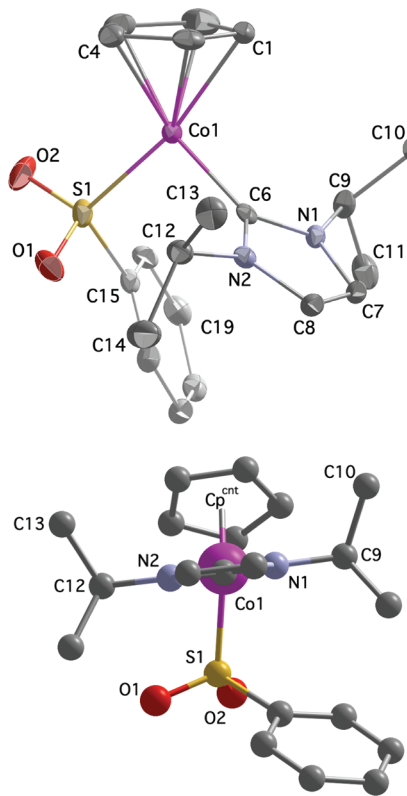


Figure 9. Solid-state molecular structures of **8** (upper panel, phenyl carbons shaded a lighter color for clarity) and view of dihedral angle ($\theta = 85^\circ$) between the Cp^{cnt} -Co-C(6) and N(1)-C(6)-N(2) planes for **8** (lower panel). Hydrogen atoms have been omitted.

barrier of 13.6 kcal/mol is very close to that determined by computation (13.3 kcal/mol). In contrast, the related barrier for the analogue with methyl substituents on nitrogen, ($\eta^5\text{-C}_5\text{H}_5$) $\text{Co}(\text{PPh}_3)(\text{ImMe}_2)$, has been computed to be only 8.7 kcal/mol. Complex **5** undergoes reaction with Ph_2S_2 to give the cobaltosulfoxide complex ($\eta^5\text{-C}_5\text{H}_5$) $\text{Co}(\text{Im}'\text{Pr}_2)(\text{SPh})$ (**7**), which has been oxidized to the cobaltosulfone ($\eta^5\text{-C}_5\text{H}_5$) $\text{Co}(\text{Im}'\text{Pr}_2)(\text{SO}_2\text{Ph})$ (**8**). The solid-state structures of **5–8** have been determined by X-ray crystallography.

Experimental Section

General Data. All manipulations were performed under an atmosphere of nitrogen unless otherwise noted or in a Vacuum Atmospheres nitrogen box equipped with a Dri-Train MO 40-1 purifier. NMR spectra were recorded on a Varian Mercury

(16) Frisch, M. J.; Trucks, G. W.; Schlegel, H. B.; Scuseria, G. E.; Robb, M. A.; Cheeseman, J. R.; Montgomery, J. A., Jr.; Vreven, T.; Kudin, K. N.; Burant, J. C.; Millam, J. M.; Iyengar, S. S.; Tomasi, J.; Barone, V.; Mennucci, B.; Cossi, M.; Scalmani, G.; Rega, N.; Petersson, G. A.; Nakatsuji, H.; Hada, M.; Ehara, M.; Toyota, K.; Fukuda, R.; Hasegawa, J.; Ishida, M.; Nakajima, T.; Honda, Y.; Kitao, O.; Nakai, H.; Klene, M.; Li, X.; Knox, J. E.; Hratchian, H. P.; Cross, J. B.; Bakken, V.; Adamo, C.; Jaramillo, J.; Gomperts, R.; Stratmann, R. E.; Yazyev, O.; Austin, A. J.; Cammi, R.; Pomelli, C.; Ochterski, J. W.; Ayala, P. Y.; Morokuma, K.; Voth, G. A.; Salvador, P.; Dannenberg, J. J.; Zakrzewski, V. G.; Dapprich, S.; Daniels, A. D.; Strain, M. C.; Farkas, O.; Malick, D. K.; Rabuck, A. D.; Raghavachari, K.; Foresman, J. B.; Ortiz, J. V.; Cui, Q.; Baboul, A. G.; Clifford, S.; Cioslowski, J.; Stefanov, B. B.; Liu, G.; Liashenko, A.; Piskorz, P.; Komaromi, I.; Martin, R. L.; Fox, D. J.; Keith, T.; M. A. Al-Laham, Peng, C. Y.; Nanayakkara, A.; Challacombe, M.; Gill, P. M. W.; Johnson, B.; Chen, W.; Wong, M. W.; Gonzalez, C.; Pople, J. A. *Gaussian 03, Revision C.02*; Gaussian, Inc.: Wallingford, CT, 2004.

300 (^1H , 300 MHz; ^{31}P , 122 MHz; ^{13}C 75.5 MHz), a Varian Mercury 400 (^1H , 400 MHz; ^{31}P , 163 MHz; ^{13}C 100.7 MHz), or a JEOL 500 (^1H , 500 MHz; ^{13}C , 125.7 MHz; ^{31}P , 203.8 MHz) spectrometer. Chemical shifts were referenced to residual protio-solvent signal, and ^{31}P NMR chemical shifts were referenced to external 85% H_3PO_4 . IR spectra were recorded on a Nicolet Avatar 320 FT-IR. Benzene and hexanes were distilled over sodium/benzophenone ketyl under an atmosphere of nitrogen. All other reagents were obtained from commercial suppliers and used as received.

Computational Methods. Density functional calculations were performed using the Gaussian 03 suite of programs.¹⁶ All geometry optimizations were performed at the B3LYP/LanL2DZ¹⁷ level of theory, and single-point calculations were performed at the B3LYP/6-311G+(2d,2p) level of theory. A single geometry optimization was performed on the ($\eta^5\text{-C}_5\text{H}_5$) $\text{Co}(\text{NHC})(\text{CO})$ system using the atomic coordinates from the X-ray crystal structure. For this optimized geometry, molecular orbitals were obtained for the two fragments ($\eta^5\text{-C}_5\text{H}_5$) $\text{Co}(\text{CO})$ and NHC at the B3LYP/6-311G+(2d,2p) level of theory. The enthalpy function for rotation of the NHC ligand was obtained by performing a series of partial geometry optimizations using the carbonyl-carbon–cobalt–carbene–nitrogen (C–Co–C–N) dihedral angle as a constraint. For each resulting partially optimized structure, the energy of the system was calculated using the larger basis set defined above.

($\eta^5\text{-C}_5\text{H}_5$) $\text{Co}(\text{Im}'\text{Pr}_2)(\text{PPh}_3)$ (**5**). A toluene solution (40 mL) of ($\eta^5\text{-C}_5\text{H}_5$) $\text{Co}(\text{PPh}_3)_2$ (**1**; 1.17 g, 1.80×10^{-3} mol, 0.05 M) was added dropwise to a toluene solution (10 mL) of $\text{Im}'\text{Pr}_2$ (**19**; 0.55 g, 3.61×10^{-3} mol, 0.36 M), and the solution was allowed to stir at rt for 20 h. The volatiles were removed in vacuo, and the residue was recrystallized from toluene/hexane (1:10) to give **5** (0.67 g, 69% yield) as a dark blue powder. Mp: 190.1–191.3 °C. IR (NaCl, neat): 2972 (s), 1681 (s), 1603, 1494, 1435, 1392, 1202 (s), 1118 (s) cm^{-1} . ^1H NMR (C_6D_6): δ 0.55 (d, 6H, $J_{\text{HH}} = 6.87$ Hz, CHMe_2), 1.04 (d, 6H, $J_{\text{HH}} = 6.87$ Hz, CHMe_2), 4.74 (s, 5H, Cp), 6.32 (s, 2H, CHCH), 6.54 (sept, 2H, $J_{\text{HH}} = 6.87$ Hz, CHMe_2), 7.02 (m, 9H, PPh_3), 7.52 (m, 6H, PPh_3). ^1H NMR (C_7D_8): δ 0.54 (d, 6H, $J_{\text{HH}} = 6.95$ Hz, CHMe_2 , endo-methyl hydrogens), 1.06 (d, 6H, $J_{\text{HH}} = 6.68$ Hz, CHMe_2 , exo-methyl hydrogens), 4.65 (s, 5H, Cp), 6.34 (s, 2H, CHCH), 6.52 (sept, 2H, $J_{\text{HH}} = 6.77$ Hz, CHMe_2), 7.01 (m, 9H, PPh_3), 7.44 (m, 6H, PPh_3). $^{13}\text{C}\{^1\text{H}\}$ NMR (C_6D_6): δ 21.4 (s, CHMe_2), 24.6 (s, CHMe_2), 52.2 (s, CHMe_2), 78.4 (s, Cp), 116.4 (s, CHCH), 127.5–133.1 (PPh_3), 191.3 (d, $J_{\text{PC}} = 32.3$ Hz, Co-CNN). ^{31}P NMR (C_6D_6): δ 66.2. HRMS (FAB) for $\text{C}_{32}\text{H}_{36}\text{N}_2\text{CoP}$: [MH⁺] calculated 538.1943; found 538.1947.

($\eta^5\text{-C}_5\text{H}_5$) $\text{Co}(\text{Im}'\text{Pr}_2)(\text{CO})$ (**6**). A toluene solution of ($\eta^5\text{-C}_5\text{H}_5$) $\text{Co}(\text{CO})_2$ (**9**; 1.87×10^{-2} mol) was added dropwise to a toluene solution (20 mL) of $\text{Im}'\text{Pr}_2$ (**17**; 1.22 g, 8.01×10^{-3} mol, 0.40 M), and the mixture was heated at 35 °C for 2 days. The solution was concentrated and extracted with dry hexanes (3 × 10 mL). Removal of volatiles in vacuo gave **6** (0.73 g, 30%) as orange crystals. Mp: 182.5–184.6 °C. IR ν_{CO} : 1911 (pentane), 1911 (hexane), 1888 (CH_2Cl_2) cm^{-1} . ^1H NMR (C_6D_6): δ 1.01 (br d, 12H, CHMe_2), 4.87 (s, 5H, Cp), 5.98 (sept, 2H, $J = 6.87$ Hz, CHMe_2), 6.34 (s, 2H, CHCH). ^1H NMR ($\text{C}_4\text{D}_8\text{O}$): δ 1.01 (br s, 12H, CHMe_2), 4.88 (s, 5H, Cp), 5.99 (sept, 2H, $J = 6.69$ Hz, CHMe_2), 6.34 (s, 2H, CHCH). $^{13}\text{C}\{^1\text{H}\}$ NMR (C_6D_6): δ 22.9 (CHMe_2), 52.3 (CHMe_2), 81.0 (Cp), 117.2 (CHCH), 183.4 (CO), 208.1 (Co-CNN). HRMS (FAB) for $\text{C}_{15}\text{H}_{21}\text{N}_2\text{OCO}$: [MH⁺] calculated 304.0980; found 304.0978.

($\eta^5\text{-C}_5\text{H}_5$) $\text{Co}(\text{Im}'\text{Pr}_2)(\text{SC}_6\text{H}_5)$ (**7**). A toluene solution (3 mL) of diphenyl disulfide (59.4 mg, 0.272 mmol, 0.09 mM) was added dropwise to a toluene solution (14 mL) of ($\eta^5\text{-C}_5\text{H}_5$) $\text{Co}(\text{Im}'\text{Pr}_2)(\text{PPh}_3)$ (**5**; 293 mg, 0.544 mmol, 0.04 M), and the mixture was stirred at rt for 1 h. The volatiles were removed in vacuo, and the residue was recrystallized from a mixture of toluene/hexanes

(17) Hay, P. J.; Wadt, W. R. *J. Chem. Phys.* **1985**, 82, 299.

(1:10) to give **7** (91 mg, 87% yield) as an orange crystalline solid. μ_{eff} : 1.73 μ_B (calculated by Evans' method in CD_2Cl_2). Mp: 164.0 °C. ^1H NMR (C_6D_6): δ 3.22 ppm (br), 11.54 ppm (br). HRMS (FAB) for $\text{C}_{20}\text{H}_{26}\text{CoS}$: $[\text{MH}^+]$ calculated 385.1143; found 385.1142.

($\eta^5\text{-C}_5\text{H}_5$) $\text{Co(Im}^i\text{Pr}_2\text{)}(\text{SO}_2\text{C}_6\text{H}_5$) (8). Solid (1*S*)-(+)-(10-camphorsulfonyl)oxaziridine (36.0 mg, 0.16 mmol) was added to a toluene solution of ($\eta^5\text{-C}_5\text{H}_5$) $\text{Co(SPh)(Im}^i\text{Pr}_2$) (**7**; 20.0 mg; 5.19×10^{-2} mmol, 0.01 M) under a nitrogen atmosphere. After stirring at rt for 2 h, the volatiles were removed in vacuo and the residue was recrystallized from toluene/hexanes (1:10) to give **8** as orange crystals (10.0 mg, 48% yield). IR (NaCl, neat): 1035 cm⁻¹ (S=O). ^1H NMR (C_6D_6): δ 5.60 ppm (br), 12.76 ppm (br). HRMS (FAB) for $\text{C}_{20}\text{H}_{26}\text{O}_2\text{N}_2\text{CoS}$: $[\text{MH}^+]$ calculated 417.1042; found 417.1039.

In a separate procedure, a 20 mL round-bottom flask was charged ($\eta^5\text{-C}_5\text{H}_5$) $\text{Co(PPh}_3\text{)(Im}^i\text{Pr}_2$) (**5**; 342 mg, 0.635 mmol, 0.03 M) and dry toluene (14 mL), and a toluene solution (3 mL) of benzenesulfonothioic acid (79 mg, 0.315 mmol, 0.10 M) was added dropwise. After stirring the solution at rt for 1 h, the solution was concentrated in vacuo, and hexanes were added to

give a solid precipitate. A ^1H NMR spectrum of a representative portion of the solid mixture exhibited resonances for both ($\eta^5\text{-C}_5\text{H}_5$) $\text{Co(SPh)(Im}^i\text{Pr}_2$) (**7**) and ($\eta^5\text{-C}_5\text{H}_5$) $\text{Co(SO}_2\text{Ph)(Im}^i\text{Pr}_2$) (**8**). Orange crystals were also manually separated from the crude mixture, and an X-ray crystallographic analysis allowed a structural assignment for **8**.

Acknowledgment. Support of the National Science Foundation under CHE-0911765 and instrumentation grant CHE-0741968 is gratefully acknowledged. C.L.V. was supported by a National Science Foundation GK12 Grant (DGE-0742551). P.R.L.M. acknowledges the support of the Howard Hughes Medical Institute and Prof. J. Andrew McCammon (UCSD).

Supporting Information Available: CIF files giving details of the crystal structure determinations of **5**, **6**, **7**, and **8**. Quantum Chemistry Figures S1 and S2. This material is available free of charge via the Internet at <http://pubs.acs.org>.